# Experimental study on pyrolysis of black non-charring polymers in reduced pressure environment

Ruowen Zong[1,2], Ruxue Kang[1]

[1] State Key Laboratory of Fire Science, University of Science and Technology of China
Huang Shan Road 443, Hefei, Anhui Province, P.R. China

[2] Suzhou Key Laboratory of Urban Public Safety, Suzhou Institute for Advanced Study, University of Science and Technology of China, Suzhou, Jiangsu, 215123 China
E-mail: zongrw@ustc.edu.cn

## Abstract

In order to study the pyrolysis of opaque non-charring polymers in the reduced pressure environment, a series of experiment on the opaque Acrylonitrile Butadiene Styrene(ABS) in reduced low-pressure chamber has been conducted under different external heat fluxes in this work . The temperatures for the surface and bottom of the sample and the mass loss during the whole process have been measured. The parameter of $T_P$, which describes the impact of pressure on the sample surface temperature has been introduced. The char residue has been observed. The results shows that under the low heat flux, there is a loose layer of char residue left with significant pyrolysis bubbles in it, and the size of the bubbles decreases with the pressure. $T_P$ has been indicated with the trend of significant decline as the pressure increased, and the mass loss rate of the sample decreases apparently as the pressure increased. While, under the high heat flux, the char residue is denser, and the pyrolysis bubbles cannot be found. $T_P$ and the mass loss rate of sample have no obvious relationship with pressure. The average pyrolysis rate is linearly related to $p^a$. The value of $a$ is 1.3 under 18kW/m², and 0.1 under 36kW/m².

*Key words:* Reduced pressure, Surface temperature, Bottom temperature, Mass loss rate, Char residue

## Nomenclature

| | |
|---|---|
| $a$ | constant |
| $C$ | specific heat at constant pressure |
| $h$ | heat convective coefficient |
| $Gr$ | Grashof number |
| $\dot{m}''$ | mass loss rate |
| $\dot{m}$ | combustion rate |

| $Pr$ | Prandtl number |
|------|----------------|
| $p$ | ambient pressure |
| $T_P$ | pressure characteristic temperature |
| $T$ | temperature |
| $\vec{u}$ | gas velocity |

**Greek symbols**

| $\rho$ | density |
|--------|---------|
| $\kappa$ | permeability |
| $\mu$ | viscosity |

**Subscript**

| $s$ | solid phase |
|-----|-------------|
| $g$ | gaseous phase |
| $v$ | volatiles |

## 1    Introduction

In recent years, polymer has been widely used in the industry and life for their characteristics of low-cost and lightweight. However, the huge amount of C, H atoms in the polymer make it high flammable and great danger to burn[1]. The study on combustion behavior of polymers is of great importance. Pyrolysis is the first step in gasification and in other thermochemical conversion processes[2].The investigation of the influence of operating conditions on the pyrolysis behaviors is important for the study of the whole combustion process.

Some materials, like polypropylene(PP), poly(lactic acid) (PLA), and poly(acrylonitrile butadiene styrene)(ABS) were classified as non-charring materials, which residual mass obtained from heating mg-sized samples at the temperature range from RT to 873 K in an anaerobic environment was found to be below 5%[1]. These materials' pyrolysis process will take place in airplane, spacecraft and low-pressure and high-altitude environment. The ambient pressure in the high-altitude area is lower than atmospheric pressure. The Chinese city of Lhasa has an altitude of 3650m, and an ambient pressure of 67kPa, which is 34% lower than the atmospheric pressure (101kPa, 21%$O_2$). And according to the Rule of Federal Aviation Administration(FAA), the pressure in the cabins of spacecraft equals to that of the place where the altitude is 1500-2400m[3, 4]. The pressure is related with the pyrolysis process in polymers' gasification and heat convection. Much attention has been paid to the pyrolysis behavior in vacuum or atmospheric pressure environment. Li et al[5] conducted some atmosphere-controlled, radiation-driven gasification experiments on a series of synthetic polymers, measured the mass loss rate, non-radiation surface temperature, conducted the thermogravimetric(TGA) and differential scanning calorimeter(DSC) and subsequently completed pyrolysis models. Mork et al[6] used a stainless steel pressure vessel connected with DSC to investigate the effect of pressure on the heat demands of cellulose pyrolysis, and pointed out that high pressure reduced the heat of pyrolysis and increased char formation. Some studies have been made in the low-pressure and poor-oxygen environment, but the key points were focused on the combustion of fuel pool or the fire spread of polymers. Liang et al[7]    conducted some experiments on the poly(methyl methacrylate) to study the effects of altitude and intersection angle on the flame spread behavior and pyrolysis front

characteristics along corner walls. It pointed out that the high altitude led to a spread rate about half of that at the lower altitude both for upward and lateral spread irrespective of the intersection angle. Qie et al[8] conducted some experiments on the wood to investigate the influence of orientation and altitude on the pyrolysis and ignition characteristic of wood. The results pointed out that there were shorter ignition times, faster mass loss rate, and higher surface temperatures in Lhasa than in Hefei. Hu et al[9] conducted a set of n-heptane pool fire experiments in Lhasa and Hefei to study the combustion and smoke characteristics at different altitudes and found that with the increase of altitude, burning rate per area and average flame axis temperature decrease. So far, there are few researches focused on pyrolysis behaviors in reduced-pressures on non-charring polymers. In this work, a series of experiments on the black poly(Acrylonitrile Butadiene Styrene)(ABS) in the reduced low-pressure chamber has been conducted to study the pyrolysis of this polymer under different external heat fluxes. Delichatsios et al[10] found that for black non-charring polymers, the transmittance is less than 0.003 when the thickness is beyond 3mm. This paper assumed that the sample as opaque. The temperature for the surface and bottom of the sample and the mass loss during the whole process have been measured in real time. The parameter of $T_P$, which describes the impact of pressure to the sample surface temperature is introduced. In addition, the char residue has been observed.

## 2  Experiments

The experiments were conducted in an intelligent low-pressure lab chamber of the State Key Laboratory of Fire Science (SKLFS) in University of Science and Technology of China (USTC). The setup is established manually to simulate the low-pressure environment. The volume fraction of $O_2$ has been controlled at the range of 4%-5%. Fig.1 shows the schematic of the pyrolysis setup.
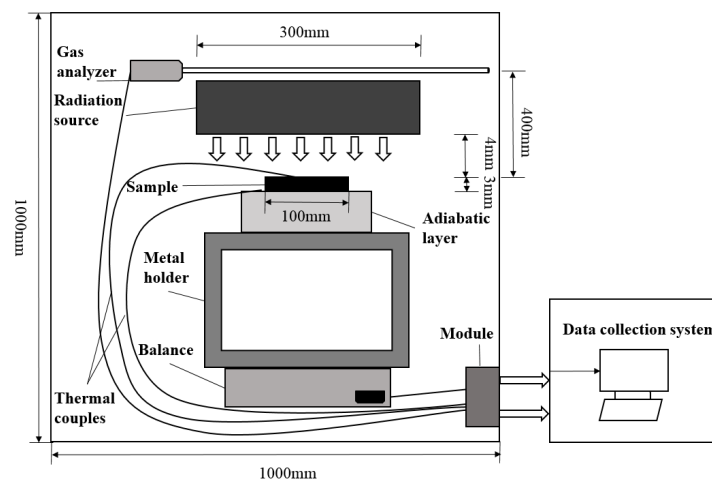


Fig.1 Schematic of the experimental setup

The intelligent low-pressure lab cabin is composed of three main parts: the pressure control system, the vacuum pump and the lab chamber. $N_2$ is injected into the chamber through the tube under the chamber. The pyrolysis setup is composed of 6 items: the radiation source, heat flow meter, electronic scale, thermal couples gas analyzer and the data collection system. The samples are black ABS sheets whose sizes are all 100mm×100mm×3mm. To assure the one-dimension pyrolysis process, all sides

and the bottom of samples have been covered by aluminized paper. And all the paper are 10mm higher than the samples surfaces with the consideration of the thermal expansion of samples. The 0.5mm K-type thermal couples have been fixed on and under the samples to measure the surface and bottom temperature respectively. According to three pre-experiments, the error of temperature is less than 6%. An asbestos plate is set under samples to create an adiabatic bottom condition. The gas analyzer is set 400mm above the samples to measure the change of contents of $O_2$ in real time. The pressure of the chamber is decreased to 25kPa at first by using the vacuum pump, then $N_2$ is injected into the chamber to rise the pressure up to the natural pressure. Then, the vacuum pump is reset to reduce the pressure to the work pressure. This paper has set five types of work conditions and each condition has its own work pressure, which is presented in Tab.1.

Table.1 Work circumstances and its corresponding pressure

| Area | Altitude[m] | Pressure[kPa] |
| --- | --- | --- |
| Condition 1(Hefei)* | 29.8 | 98.1 |
| Condition 2(Sining) | 2158.6 | 77.4 |
| Condition 3(Lhasa) | 3259.4 | 65.2 |
| Condition 4 | 4179.7 | 55.0 |
| Condition 5 | 5984.2 | 35.0 |

*means the atmospheric pressure.

Radiation heat fluxes are controlled by the heat flow meter. The external radiation source is fixed at the far left of a slide way in the cabin. It is put right above the sample by a heavy iron block until the radiation heat flux went stable. The sample has been set right under the center of the radiation source. The size of the source is 300mm×300mm, and the distance between the source and the sample was 40mm. The test heat fluxes were 18kW/m$^2$ and 36kW/m$^2$. The samples weighted before tests. The test is not finished until the pyrolysis mass loss was larger than 95% of the original mass.
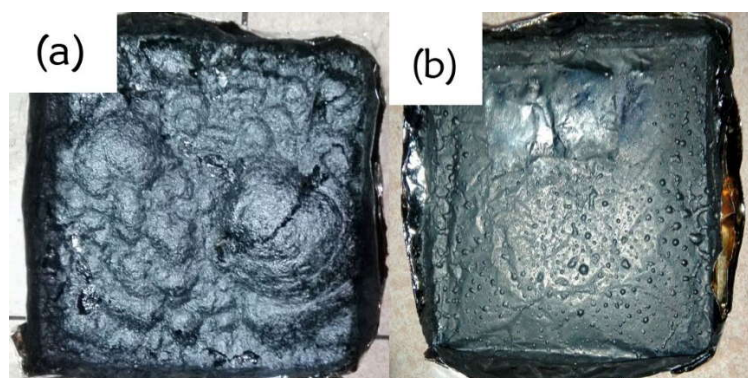
## 3    Results and Discussion

### 3.1 Char residues



Fig. 2 Char residues of samples under different heat fluxes in 98.1kPa environment:

(a)18kW/m$^2$   (b)36kW/m$^2$

Figure 2 shows the effect of heat fluxes on the char residues in the environment of 98.1kPa. Apparently, under the lower heat flow of 18kW/m$^2$, there is a loose layer of char residue left after the

pyrolysis, and some bubbles appears due to the escape of pyrolysis gas. While under the higher heat flow of 36kW/m$^2$, the char residue of ABS is denser. Under the lower heat flow, the pyrolysis rate of ABS is slower, so the surface and the inner part of the sample starts to pyrolysis almost at the same time. In addition, the bottom of the sample is on the condition of heat insulation, so the inner temperature becomes higher than the surface temperature after a certain time, leading to a faster pyrolysis rate inside the sample. The inside pyrolysis gas escapes through the sample surface and causes some bubbles. Under higher heat flow, the pyrolysis rate is faster and the high heat flow leads to thermal hysteresis. The higher the heat flow is, the more obvious the thermal hysteresis is[11-13]. Thermal hysteresis makes the pyrolysis of samples carry through layer by layer. Under a higher heat flow, the end of the pyrolysis on the surface is earlier than that on the inner part, which results in a denser and non-bubbles char residue layer.
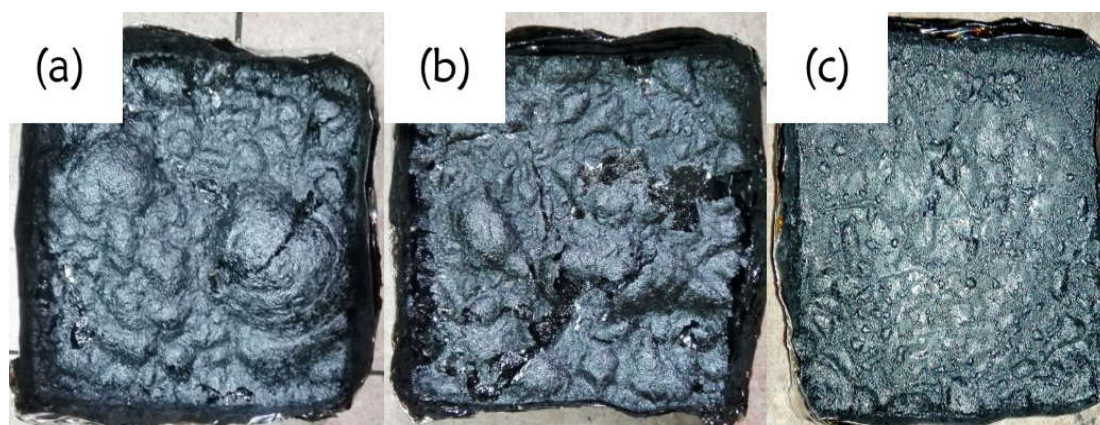


Fig. 3 Char residues of samples in different pressure environment under 18kW/m$^2$:

(a)98.1kPa    (b)65.2kPa    (c)35kPa

Figure 3 shows the influence of pressure to the char residues under 18kW/m$^2$. Apparently, the sizes of pyrolysis bubbles get smaller and smaller with the decrease of the pressure. The reason is that the pressure, which is related to transformation of the convective heat, will rise the sample's temperature during the pyrolysis process (More details will be discussed later.). The rise of temperature results in a faster pyrolysis rate on the surface. The decrease of pressure makes the pyrolysis gases easier to escape, which keeps gases from gathering inside of the sample. So the bubbles become smaller.

## 3.2 Surface and bottom temperature

Quintiere[14] points out that the temperature of pyrolysis gas releasing from the sample's inside is identical with that of the sample's surface, so the gas temperature can be decided by measuring the temperature of the surface. Fig.4 shows that under an external heat radiation, the temperature of surface will suddenly jump to a certain value and then rise slowly. Here the temperature value has been defined as the pressure characteristic temperature, denoted as $T_P$, as shown in the Fig.4(a). In this process, the heat absorbed by polymers in succession has been distributed to heat conduction, heat convection, heat radiation and samples' pyrolysis processes. However, in the different pressure environment, under different heat flows, $T_P$ and the profiles of surface temperatures behave differently. Obviously, under

18kW/m² heat flow , the values of $T_P$ show the trend of significant decrease with the increase of pressure; whereas, under 36kW/m² heat flow, the decrease of $T_P$ can be neglected.
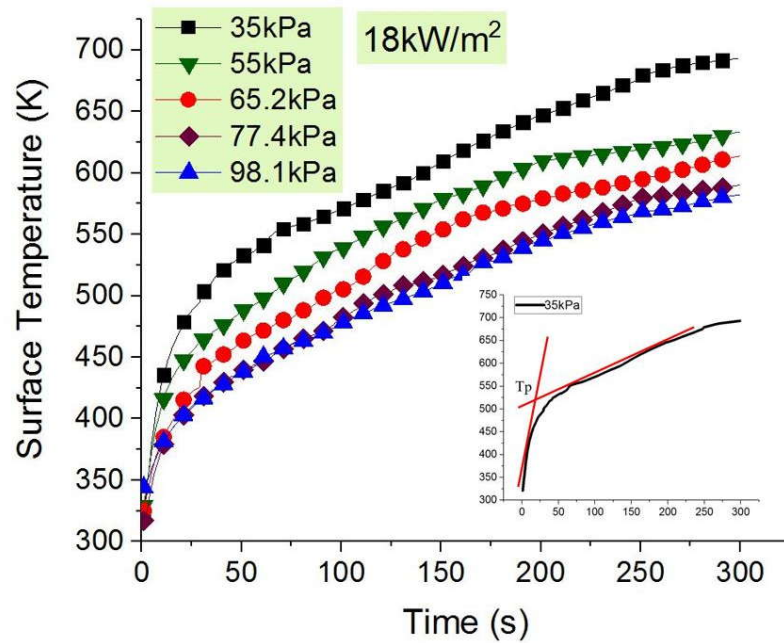


(a)
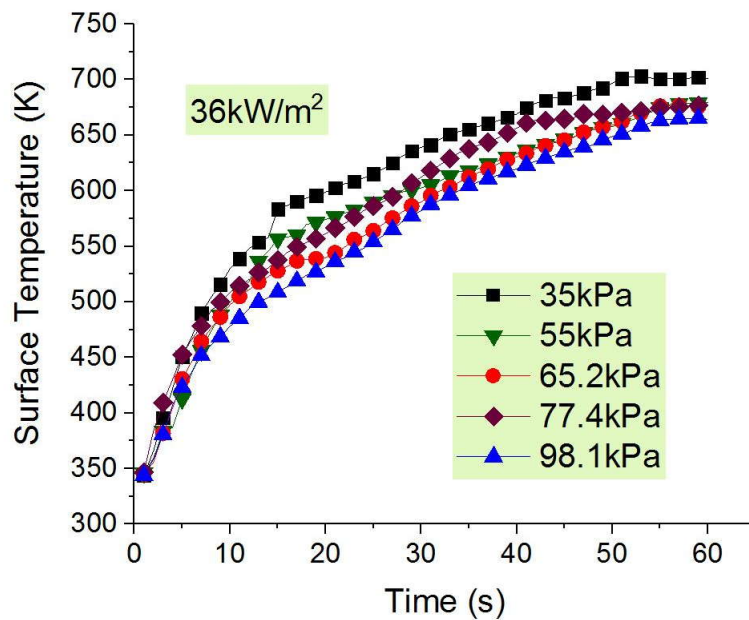


(b)

Fig.4 Profiles of the surface temperature under different pressures: (a)18kW/m² (b)36kW/m²

Under natural situations, the convective heat transfer coefficient is related to some parameters, which is shown as follows[15]:

$$h \propto Gr^{1/4} Pr^{1/4} \qquad (1)$$

Where $Gr$ is the Grashof number, $Pr$ is the Prandtl number. $h$ is the heat convective coefficient.

As shown in Eq.(1), $Gr$ is proportional to the square of the pressure, so the convective heat transfer coefficient is proportional to the square root of the pressure. The higher pressure is, the bigger convective heat transfer coefficient is, and vice versa. The surface control volume of the sample contacts with air directly, and the heat and mass transfer processes exist. The energy-balance equations are as follows[16]:

$$\rho_s C_s \frac{\partial T_s}{\partial t} = \tau \dot{q}_{ext}^{"} - \varepsilon_{pol} \sigma (T_s^4 - T_\infty^4) - h_{conv}(T_s - T_\infty) + k_s \frac{\partial T_s}{\partial x} - Q_{out} \qquad (2)$$

$$Q_{out} = \rho_s S_v [\Delta H_v + (T_S - T_\infty)(C_s - C_g)] + \dot{m}^{"} C_g \frac{\partial T_s}{\partial x} \qquad (3)$$

Where $\rho$ is the density, $C$ is the specific heat at constant pressure, $T$ is the temperature, $\dot{m}^{"}$ is the mass loss rate. The subscript of $s$, $g$, $v$ is the solid phase, gaseous phase and volatiles respectively.

Equation (2) and (3) show that under certain heat flow, the convective heat loss increases with the convective heat transfer coefficient, but $T_P$ decreases as the convective heat transfer increases. Under lower heat flow, the inflow energy of the surface is relatively less, so the convective heat transfer coefficient has a bigger impact on the surface temperature of samples. Thus, pressure has a significant impact on $T_P$. While under higher heat flow, the inflow energy of the surface is much more, so the convective heat transfer coefficient has a negligible influence, and the change of $T_P$ can be neglected.
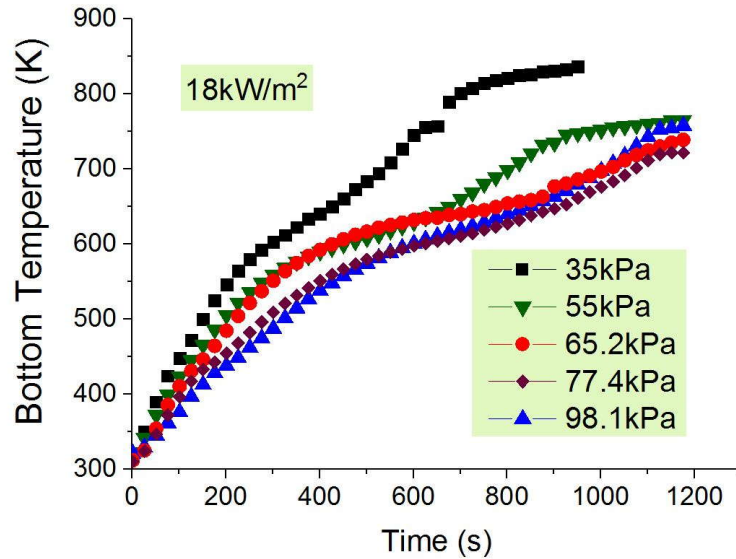


(a)
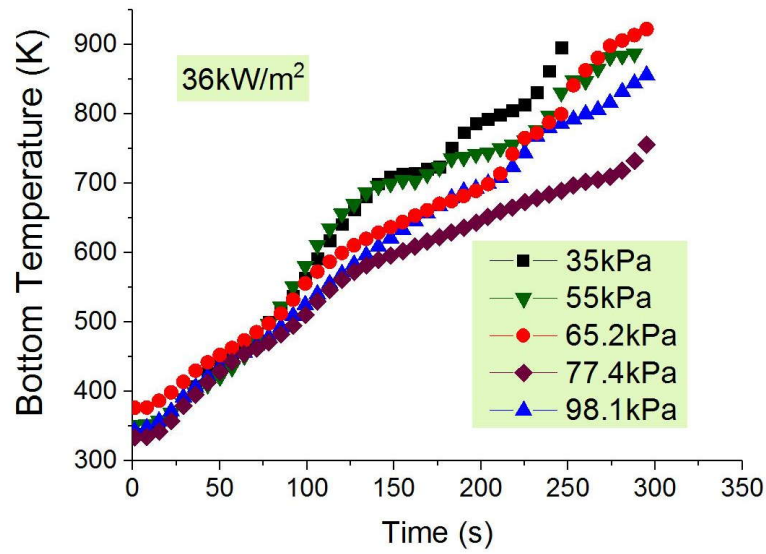
(b)

Fig.5 Profiles of the bottom temperature under different pressures: (a)18kW/m$^2$ (b)36kW/m$^2$

Figure 5 shows that different heat flows have different impacts on the bottom temperatures of sample. Obviously, at the pressure of 35kPa, the pyrolysis ended earlier than that in the other pressures. The curves cannot present the starting point of the pyrolysis process, but under lower heat flow, the massive pyrolysis time of sample can be observed. The massive pyrolysis starts at the time when the temperature increase ratio reaches gentle after a rapid increase. Then the bottom temperature rises slowly and the inflow energy has been consumed greatly in the pyrolysis process. Under higher heat flow, the outflow energy is quite small, so the temperature keeps rising until the sample's pyrolysis ends. The pressure has similar impact on the bottom temperature with that on the surface temperature. However, the bottom temperature is less sensitive to pressure than the surface temperature. The reason is that on the condition of heat insulation, the inside and the bottom parts of samples have little heat convective loss. Under the higher heat flow, the loss is negligible, so its bottom temperature change is not obvious as the pressure changes.

## 3.3 Mass loss rate
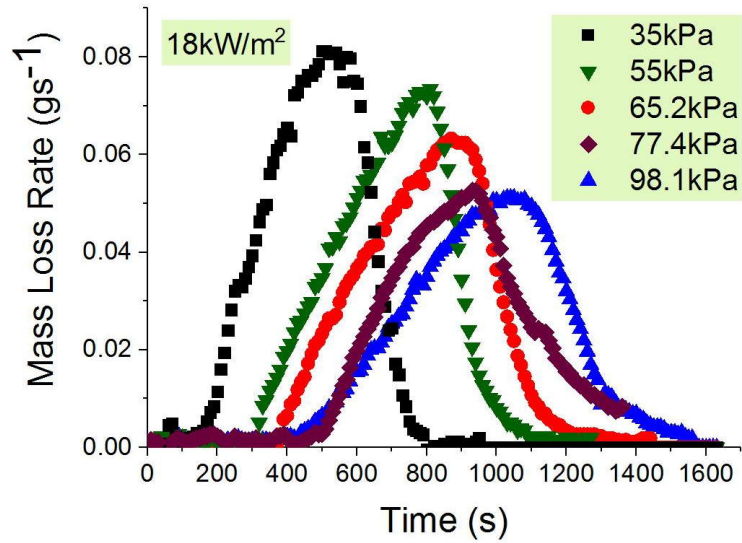
(a)
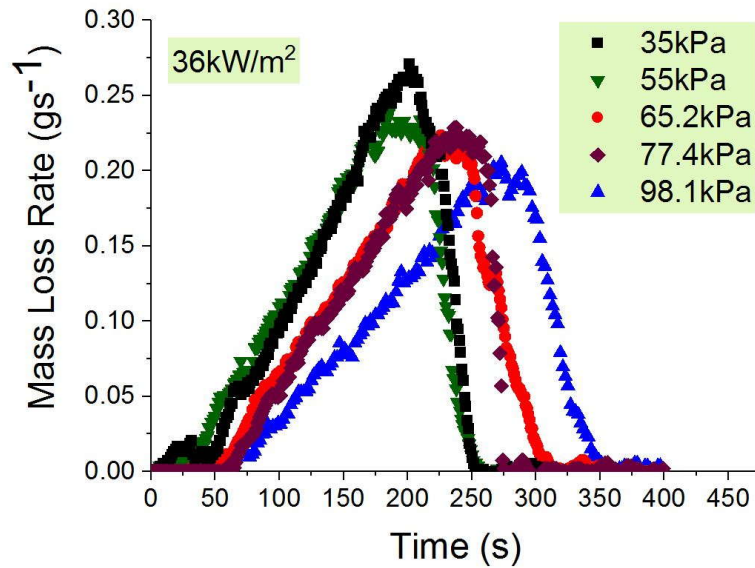


(b)

Fig.6 Profiles of the mass loss rate under different pressures: (a)18kW/m$^2$(b)36kW/m$^2$

The profiles of the mass loss rate under different gas pressures is shown in Fig.6. Obviously, the external radiation intensity has significant impact on the mass loss rate. Under 18kW/m$^2$ heat flow, the mass loss process mainly takes place between 200-1400s; while under 36kW/m$^2$ heat flow, the period of mass loss process has been moved ahead to 50-350s. Under lower heat flow, the mass loss rate(MLR) shows a higher sensitivity to the pressure, and MLR decreases as the pressure goes up. The reason is that the sample's gross heat loss decreases with the convective heat transfer coefficient, and the decrease of heat loss influences the sample's net absorbed heat obviously. So MLR increases as the pressure goes down. For the sample under 98.2kPa, the climax of MLR occurs at the time around 1050s when the temperature is 418.5℃, which is nearly identical with the results of Sonia Fereres et al[17].

In addition, Di Blasi et al[18, 19] point out that the Darcy Law describes how the pressure influences the pyrolysis gases' flow inside solid materials. According to the Darcy Law, the velocity equation of the gas flow is shown as follows:

$$\vec{u} = -\frac{\kappa_D}{\mu}\frac{dp}{dx} \tag{4}$$

Where $\vec{u}$ is the gas velocity, $K_D$ is the permeability, $\mu$ is the viscosity.

As shown in Eq.(4), the larger the pressure gradient is, the faster the gas velocity is. As the pressure goes down, the pressure gradient inside the sample and the air goes up, which leads to a faster gas release rate from the inside of the sample. So MLR increases.

Wieser et al[20] describes that the relationship between the combustion rate $\dot{m}$ and the ambient pressure $p$ is as follow:

$$\dot{m} \propto p^a \tag{5}$$

Where $a$ is constant, and the value of $a$ reflects the sensitivity of pyrolysis rate to the pressure.

This work takes the pyrolysis stage between 2%-95% of the total pyrolysis process to decide the average pyrolysis rate. Then, the relationship between them can be fitted linearly.
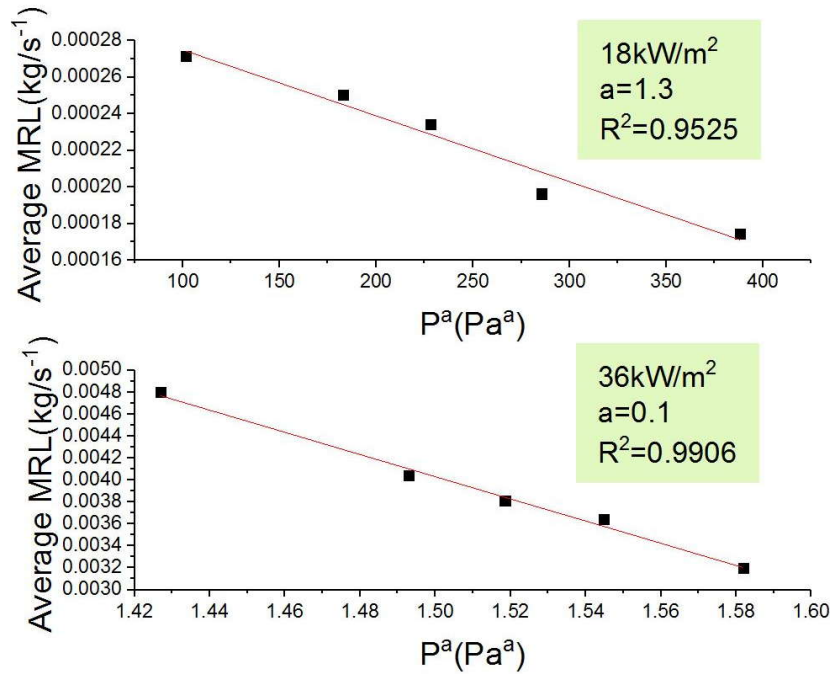


Fig.7 Profiles of average MRL with different Pa under different heat flows

As shown in Fig.7, for the same sample, different intensity heat flows impose different impacts on the pyrolysis rate. Under 18kW/m², $a = 1.3$, which means under lower heat flow, the pyrolysis rate has more sensitivity to the pressure. Under the heat flow of 36kW/m², $a = 0.1$, which means under higher heat flow, the pyrolysis rate has little sensitivity to the pressure.


## 4 Conclusions

This work has conducted a series of experiment on the black poly(Acrylonitrile Butadiene Styrene)(ABS) in reduced low-pressure chamber to study the pyrolysis of black non-charring polymers under different external heat fluxes. The temperature for the surface and bottom of the sample and the mass loss during the whole process have been measured in real time. The parameter of $T_P$, which

describes the impact of pressure on the sample surface temperature is introduced. In addition, the char residue has been observed. The conclusions are as follows:

a. Under the lower heat flow, there is a loose layer of char residue left after the pyrolysis, and in addition, there are some bubbles in it due to the escape of the pyrolysis gas. While under higher heat flow, the char residue of ABS is denser without obvious bubbles on it. Under the lower heat flow, the size of pyrolysis bubbles goes smaller and smaller with the decrease of the pressure.

b. In the different pressure environment, under different heat flows, $T_P$ and the profiles of surface temperatures behave different. $T_P$ shows the trend of significant decrease as the pressures go up under lower heat flow. While, under higher heat flow, the decreases of $T_P$ are negligible. The pressure has similar impact on the bottom temperature with that on the surface temperature.

c. Under lower heat flow, MLR shows a high sensitivity to the pressure, and MLR decreases as the pressure goes up. While under higher heat flow, MLR shows a negligible sensitivity to the pressure. The pyrolysis rate $\dot{m}$ is proportional to the $a^{th}$ power of the ambient pressure $p$. For 18kW/m$^2$, $a = 1.3$. for 36kw/m$^2$, $a = 0.1$.

## Acknowledgments

## References

[1] LI J, STOLIAROV S I. Measurement of kinetics and thermodynamics of the thermal degradation for non-charring polymers [J]. Combustion and Flame, 2013, 160(7): 1287-97.

[2] BASILE L, TUGNOLI A, STRAMIGIOLI C, et al. Influence of pressure on the heat of biomass pyrolysis [J]. Fuel, 2014, 137(277-84.

[3] LANGE K, PERKA A, DUFFIELD B, et al. Bounding the spacecraft atmosphere design space for future exploration missions. 2005 [J]. National Aeronautics and Space Administration, NASA/CR-2005-213689,

[4] MCALLISTER S, FERNANDEZ-PELLO C, URBAN D, et al. Piloted ignition delay of PMMA in space exploration atmospheres [J]. P Combust Inst, 2009, 32(2): 2453-9.

[5] LI J, GONG J H, STOLIAROV S I. Development of pyrolysis models for charring polymers [J]. Polym Degrad Stabil, 2015, 115(138-52.

[6] MOK W S L, ANTAL M J. Effects of Pressure on Biomass Pyrolysis .2. Heats of Reaction of Cellulose Pyrolysis [J]. Thermochimica Acta, 1983, 68(2-3): 165-86.

[7] LIANG C J, CHENG X D, LI K Y, et al. Experimental study on flame spread behavior along poly(methyl methacrylate) corner walls at different altitudes [J]. J Fire Sci, 2014, 32(1): 84-96.

[8] QIE J, YANG L, WANG Y, et al. Experimental study of the influences of orientation and altitude on pyrolysis and ignition of wood [J]. J Fire Sci, 2011, 29(3): 243-58.

[9] HU X-K, HE Y-P, LI Z-H, et al. Combustion and Smoke Characteristics of Circle-Pan Fire Under Low Pressure and Low Oxygen Concentration [J]. Journal of Combustion Science and Technology, 2011, 2(005.

[10] DELICHATSIOS M, SAITO K. Upward fire spread: key flammability properties, similarity solutions and flammability indices [J]. Fire Safety Science, 1991, 3(217-26.

[11] HULBERT S. Models for solid-state reactions in powdered compacts-- a review [J]. J Brit Ceram Soc, 1969, 6(1): 11-20.

[12] SHARP J, BRINDLEY G, ACHAR B N. Numerical data for some commonly used solid state reaction equations [J]. Journal of the American Ceramic Society, 1966, 49(7): 379-82.

[13] GIESS E A. Equations and Tables for Analyzing Solid-State Reaction Kinetics [J]. Journal of the American Ceramic Society, 1963, 46(8): 374-6.

[14] QUINTIERE J. A theoretical basis for flammability properties [J]. Fire Mater, 2006, 30(3): 175-214.

[15] MCALLISTER S, FERNANDEZ-PELLO C, URBAN D, et al. The combined effect of pressure and oxygen concentration on piloted ignition of a solid combustible [J]. Combustion and flame, 2010, 157(9): 1753-9.

[16] INCROPERA F P, DE WITT D P. Fundamentals of heat and mass transfer [J]. 1985,

[17] FERERES S, LAUTENBERGER C, FERNANDEZ-PELLO C, et al. Mass flux at ignition in reduced pressure environment [J]. Combustion and flame, 2011, 158(7): 1301-6.

[18] KANSA E J, PERLEE H E, CHAIKEN R F. Mathematical model of wood pyrolysis including internal forced convection [J]. Combustion and Flame, 1977, 29(311-24.

[19] DI BLASI C. Modeling and simulation of combustion processes of charring and non-charring solid fuels [J]. Progress in Energy and Combustion Science, 1993, 19(1): 71-104.

[20] WIESER D, JAUCH P, WILLI U. The influence of high altitude on fire detector test fires [J]. Fire Safety J, 1997, 29(2-3): 195-204.